Transmission electron microscopic observation of a metastable phase on the thermal decomposition process of Ca-deficient hydroxyapatite

MASATO TAMAI*
Department of Chemistry and Materials Technology, Kyoto Institute of Technology, Gosho-kaido-cho, Matsugasaki,, Sakyo-ku, Kyoto 606-8585, Japan
E-mail: m-tamai@nihs.go.jp

TOSHIYUKI ISSHIKI, KOJI NISHIO, MITSUHIRO NAKAMURA
Department of Electronics and Information Science, Kyoto Institute of Technology, Gosho-kaido-cho, Matsugasaki,, Sakyo-ku, Kyoto 606-8585, Japan

ATSUSHI NAKAHIRA
Department of Chemistry and Materials Technology, Kyoto Institute of Technology, Gosho-kaido-cho, Matsugasaki,, Sakyo-ku, Kyoto 606-8585, Japan

HISAMITSU ENDOH
Department of Electronics and Information Science, Kyoto Institute of Technology, Gosho-kaido-cho, Matsugasaki,, Sakyo-ku, Kyoto 606-8585, Japan

Published online: 12 January 2006

Calcium-deficient hydroxyapatite (Ca-def HAp) decomposes to stoichiometric hydroxyapatite (HAp) and β-tricalcium phosphate (β-TCP) at high temperature. In a previous study, we reported that a metastable phase with a high Ca/P molar ratio appeared in the temperature range from 700 to 800°C. In the present study, the formation process of a metastable phase and the crystallographic relationship between the Ca-rich metastable phase and HAp matrix were investigated by high-resolution transmission electron microscopy (HRTEM). Ca-def HAp was annealed at 600–850°C for 2 or 6 h in air. TEM observations were performed before and after annealing Ca-def HAp. Based on analysis of image of Ca-def HAp before annealing, several HAp crystals with different aspect ratios agglomerated. The metastable phases grew thicker by long-term annealing. HRTEM image suggested that the Ca-rich metastable phase was formed by migration to the interface and continuous accumulation of calcium ions from HAp crystals with a small aspect ratio. From HRTEM images and results of the analysis of selected area electron diffraction patterns along the [010], [110] and [001] zone axes, lattice constants of the metastable phases were determined to be $a = 2.86$ nm, $b = 0.94$ nm, and $c = 0.69$ nm with orthorhombic crystals system.

1. Introduction

Calcium-deficient hydroxyapatite (Ca-def HAp, $Ca_{10-Z}(HPO_4)_Z(PO_4)_{6-Z}$ $(OH)_{2-Z}$, $Z = 0$–1) has a Ca/P ratio lower than that of stoichiometric HAp ($Ca_{10}(PO_4)_6(OH)_2$, hexagonal, $a = 0.943$ nm, $c = 0.688$ nm; space group: $P6_3/m$). Ca-def HAp is of greater biological interest than stoichiometric HAp since the Ca/P molar ratio in bone is lower than 1.67. It has been suggested that Ca-def HAp plays important roles in several processes, such as bone remodeling and bone formation [1].

Ca-def HAp decomposes to stoichiometric HAp and β-tricalcium phosphate (β-TCP, β-$Ca_3(PO_4)_2$, rhombohedral, $a = 1.044$ nm, $c = 3.738$ nm

*Author to whom all correspondence should be addressed.
0022-2461
DOI: 10.1007/s10853-005-2458-x

(hexagonal setting); space group: R3c) at more than 600°C [2, 3]. The thermal decomposition of Ca-def HAp is very important for biomaterials design, since an HAp/β-TCP biphasic composite with high biocompatibility can be fabricated easily by a sintering process [4–6]. Although various studies on the thermal decomposition of Ca-def HAp have been carried out [7–9], the changes in microstructure during thermal decomposition have not been elucidated.

Electron microscopy is a useful tool to investigate the microstructure of the various materials. For example, Rosen and co-workers investigated the nucleation of HAp during the mineralization process in bone remodeling by transmission electron microscopy (TEM), and showed that the mineralization of collagen comprising osteoid proceeds by the formation of HAp crystallites within the fibers at selected periodic sites [10]. On the other hand, we have focused on microstructure changes on an atomic length scale during the thermal decomposition process of Ca-def HAp, which we have investigated by high-resolution transmission electron microscopy (HRTEM). We found a metastable phase with a high Ca/P molar ratio in the temperature range from 700 to 800°C [11]. A precipitation parallel to the (100) plane of the HAp matrix was observed in the samples annealed at 700 and 800°C. The thickness of the precipitation was about 10 nm and the boundaries between the precipitation and HAp matrix were coincident. Since the precipitation was observed only in the sample annealed at a narrow temperature range of 700–800°C, it was regarded as a metastable phase formed during the thermal decomposition process. Furthermore, the results of energy dispersive X-ray spectroscopy showed that the metastable phase had a Ca/P molar ratio higher than that of the matrix and stoichiometric HAp. In the present study, we investigated the formation process of the metastable phase and the crystallographic relationship between the metastable phase and HAp matrix by HRTEM.

2. Experimental procedures

Ca-def HAp was prepared by hydrolysis of α-TCP [11] (Taihei Chemical Industries, Co., Ltd. Nara, Japan). 0.01 mol of α-TCP was stirred for 48 h at 70°C in 1-octanol/H_2O binary solvent (100 ml/60 ml). The pH of the binary solvent was adjusted to 11.0 by ammonia aqueous solution. The sample was filtrated, washed with ethanol three times, and dried at 50°C for 24 h. The Ca-def HAp was annealed at 700–850°C in air (heating rate: 5°C /min). In order to investigate the formation mechanism of the metastable phase, the duration of annealing was set to 2 or 6 h.

Ca-def HAp crystals before and after annealing were identified by powder X-ray diffraction (XRD) analysis using a RINT 2000 diffractometer (Rigaku Co., Ltd., Tokyo, Japan) with the Cu K_α radiation at 40 kV, 50 mA. The XRD profiles were collected between 20–60° of 2θ angles with a step interval of 0.01° and scanning rate of 4°/min. The Ca-def HAp crystals before and after annealing were also identified by infrared absorption spectroscopy analysis (IR: IR-WINSPEC100; JEOL, Tokyo, Japan). The atomic concentrations of calcium and phosphorus in the Ca-def HAp before annealing were measured by inductive coupled plasma (ICP: ICAP9000; Janell-Ash). Ca-def HAp crystals before and after annealing were mounted on a Cu grid with a carbon-coated holey film for TEM by dripping the ethanol suspension of the sample. TEM observations were carried out with a JEOL JEM-2010SP (accelerating voltage: 200 kV). TEM observations were performed along [010], [110] and [001] zone axes in order to investigate the structure of the metastable phase and the relationship between the metastable phase and HAp matrix.

3. Results and discussion

From the results of XRD, IR and ICP analysis, the Ca-def HAp prepared by the hydrolysis method was identified as well-crystallized Ca-def HAp with a Ca/P molar ratio of 1.58 [12]. TEM images of Ca-def HAp before annealing are shown in Fig. 1. Ca-def HAp synthesized by the hydrolysis method has a whisker-like morphology elongated along the c-axis with a length of 2–5 μm and diameter of 0.1 μm. In addition, as shown in Fig. 1b, several HAp crystals with different aspect ratios agglomerated onto each other. These agglomerations of Ca-def HAp crystals grew into large crystals involving formation of the β-TCP phase at more than 700°C.

We previously reported that a metastable phase with a high Ca/P molar ratio appeared in the temperature range from 700 to 800°C [10]. Fig. 2a–c shows a whole TEM image of Ca-def HAp annealed at 800°C for 2 h; the Ca-rich metastable phase, is shown in Fig. 2a, a selected area electron diffraction (SAED) pattern is shown in Fig. 2b, and an HRTEM image of the area enclosed by a rectangle

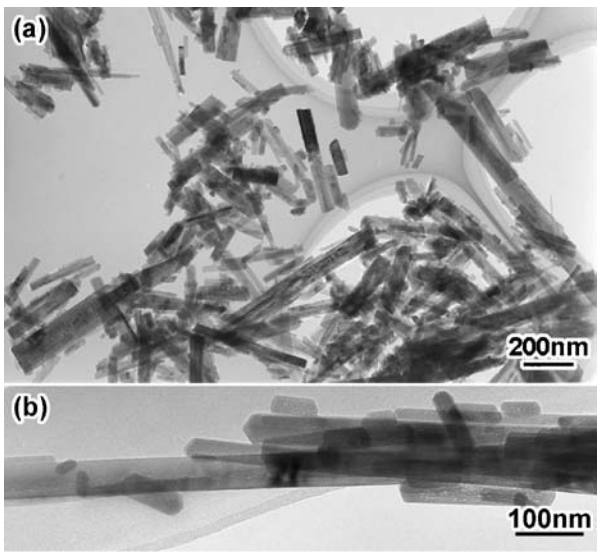

Figure 1 TEM images of Ca-def HAp prepared by hydrolysis of α-TCP: (a) Whole image and (b) enlarged TEM image.

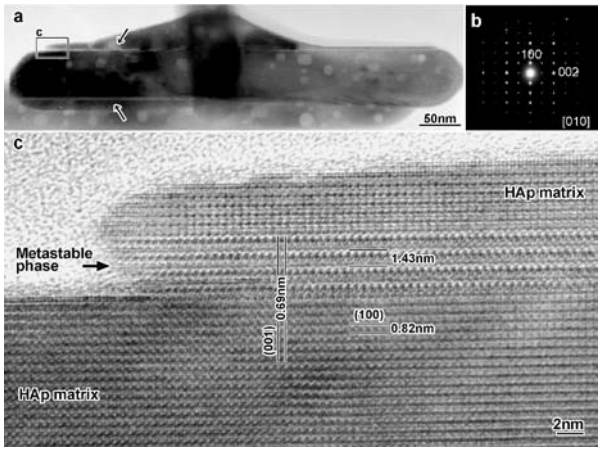

Figure 2 TEM image of Ca-def HAp annealed at 800°C for 2 h: (a) Whole TEM image, (b) selected area electron diffraction pattern and (c) HRTEM image of the area enclosed by a rectangle in (a).

in (a). A metastable phase of about 5 nm in width traverses in the HAp crystal parallel to the (100) plane of the HAp matrix, and coincident boundaries are observed between the metastable phase and HAp matrix. The periodicity in the metastable phase was parallel to the (100) plane of the HAp matrix and measured as 1.43 nm. As shown in Fig. 2a, the Ca-rich metastable phase traversed through the inside of the HAp crystal, and part of the upside of the Ca-rich metastable phase shows mountain-like morphology. From the morphology of the tip of the Ca-rich metastable phase, it appears that the two HAp crystals were originally united. As mentioned above, Ca-def HAp was originally synthesized by hydrolysis of the α-TCP agglomerate. Therefore, the boundaries between each the HAp crystals in the agglomeration will be an origin of the formation of the Ca-rich metastable phase.

A TEM image of another Ca-def HAp crystal annealed under the same annealing conditions is shown in Fig. 3a. Fig. 3b shows an enlarged TEM image of the area enclosed by a rectangle in a. As can be seen, there is a small HAp crystal of about 40 nm on a HAp whisker, and a Ca-rich metastable phase traverses under this small crystal. Here, note that the metastable phase in the left-hand side of the small HAp crystal consists of two layers with a periodicity of 1.43 nm but in the right-hand side, the metastable phase consists of five layers (Fig. 3b). The lowest layer runs just below a small HAp crystal. The TEM image also suggests that two Ca-def HAp crystals are involved in the formation of the metastable phase. In addition, as shown in Fig. 2c, a typical Ca-rich metastable phase traverses in the HAp matrix with the same number of layers, while the metastable phase confirmed in Fig. 3b consists of a few layers and a different number of layers. Therefore, the image will be an embryonic state of a metastable phase and can be interpreted as an initial stage of the formation of the Ca-rich metastable phase. Considering the fact that metastable phases have high Ca/P molar ratios, a metastable phase will be formed by the migration of calcium ions to the interfaces between Ca-def HAp crystals, and the growth will proceed by continuous accumulation of calcium ions from a HAp crystal that has a small aspect ratio and is located on a large HAp whisker. In order to verify the formation process of the metastable phase, TEM observations were performed for the samples obtained by annealing for a long period of time.

The metastable phase could not be observed in the sample annealed at more than 800°C for 6 h. In Ca-def HAp annealed at 750°C for 6 h, a metastable phase was often observed compared to a specimen annealed for 2 h. TEM images of Ca-def HAp annealed at 750°C for 6 h are shown in Fig. 4. The metastable phase becomes thicker (Fig. 4a). Furthermore, as shown in Fig. 4b, a metastable

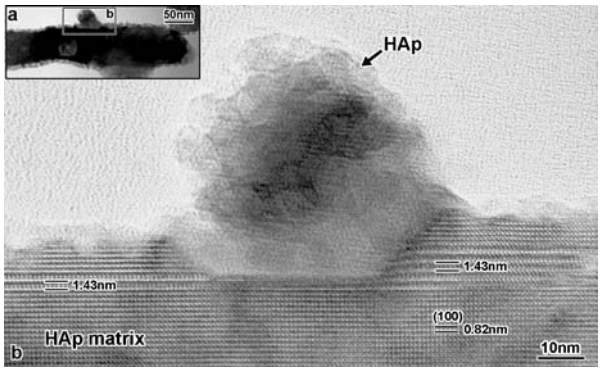

Figure 3 TEM image of Ca-def HAp annealed at 800°C for 2 h: (a) Whole TEM image, and (b) HRTEM image of the area enclosed by a rectangle in (a).

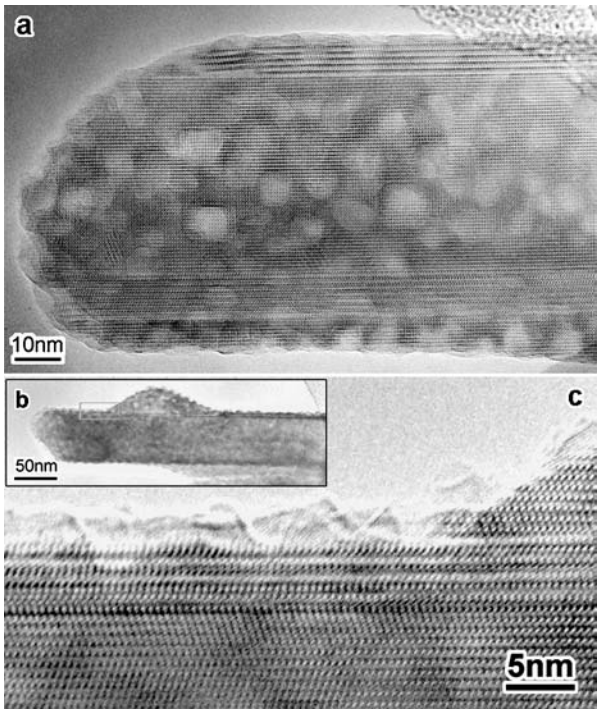

Figure 4 HRTEM image of Ca-def HAp annealed at 750°C for 6 h: Panels (a) and (b) show other samples. (c) HRTEM image of the area enclosed by a rectangle in (b).

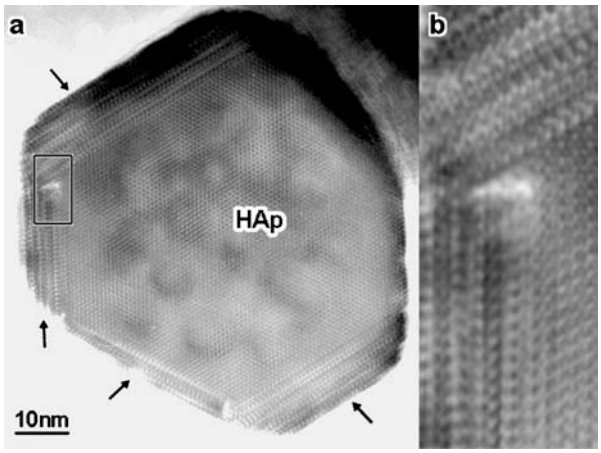

Figure 5 (a) A cross section TEM image of Ca-def HAp annealed at 750°C for 6 h (metastable phases are shown by arrows). (b) HRTEM image of the area enclosed by a rectangle in (a).

phase in Ca-def HAp annealed at 750°C for 6 h is often observed at the surface of the HAp matrix, although a metastable phase in Ca-def HAp annealed for 2 h traverses within the HAp crystal. The facts that a metastable phase is often observed and it grows thicker by annealing for a long period of time suggest that the crystal growth of the metastable phase is controlled by migration of ions or thermal diffusion at high temperatures. In addition, growth of the Ca-rich metastable phase will proceed toward the surface after an embryonic metastable phase is formed within the HAp whisker. Fig. 5 shows a cross section image of annealed Ca-def HAp containing the metastable phase. In Fig. 5a, the metastable phases can be seen around a HAp crystal. The boundaries between the metastable phases have no coherence (Fig. 5b). The cross section image suggests that a growth process in which the metastable phase grows toward the surface from the inside of the HAp matrix occurs in each side plane in the hexagonal crystal independently. Fig. 6 shows a TEM image of Ca-def HAp annealed at 750°C. As shown by

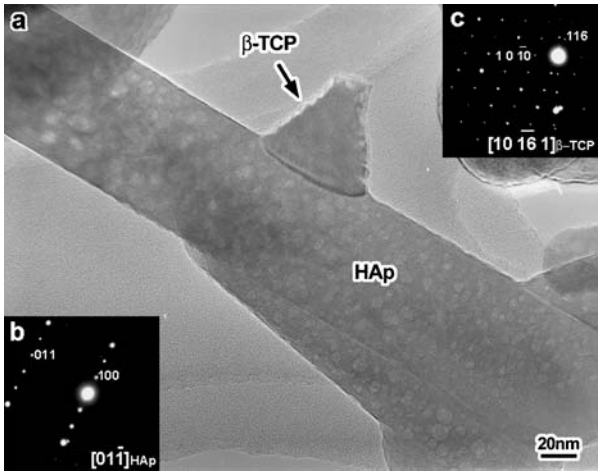

Figure 6 TEM image of Ca-def HAp annealed at 750°C for 6 h (a) and selected electron diffraction patterns (b), (c).

the SAED pattern, a β-TCP of 30 nm is on the HAp whisker. Considering the dimensions and morphology of the β-TCP, the origin of β-TCP would be a small HAp crystal that was originally present in agglomerations. As mentioned above, a metastable phase would be formed by which calcium ions migrate and accumulate to the interface between Ca-def HAp crystals. In contrast, the Ca/P molar ratio in HAp with a small aspect ratio decrease and close to 1.5, which is the stoichiometric composition of β-TCP. It is likely that the part of the apatitic structure that has a lower Ca/P molar ratio is transformed into β-TCP.

The HRTEM observation revealed that the Ca-rich metastable phase is formed by migration to the interface and continuous accumulation of calcium ions from a HAp crystal that has small aspect ratio and located on a large HAp whisker. The boundary between the metastable phase and HAp matrix has good coherence, as drastic rearrangement of atoms does not occur in the process. In this study, TEM observations along different zone axes ([010], [110] and [001]) were performed in order to investigate the structure of the metastable phase and the relationship between the metastable phase and the HAp matrix.

Figs. 7.a1, b1 and c1 shows an HRTEM image of the metastable phase along [010], [011] and [001], respectively. Figs 7a2, b2, and c3 are an SAED pattern in the region of a1b1 and c1, respectively. As shown in Figs 7a1 and c1, the spacing of the (001) plane in HAp is maintained in the metastable phase. Several diffraction spots from the metastable phase shown by arrows are observed in the SAED patterns along the [010], [110] and [001] zone axis. From the results of the analysis of SAED patterns, the lattice constants of the metastable phase were determined to be $a = 2.86$ nm, $b = 0.943$ nm, and $c = 0.69$ nm in the orthorhombic crystals system.

With respect to the relation between the HAp matrix and the metastable phase, as represented in Fig. 8, the length of the b-axis and c-axis in the metastable phase agreed with that of the b-axis and c-axis in the HAp matrix, respectively, and the (100) plane of the metastable phase ran parallel to the (100) plane of HAp matrix. Determination of the space group and atomic arrangements of the metastable phase are now in progress.

Recenty, HAp and β-TCP ceramics are used as the scaffolds for bone regeneration and their ceramics are important bioreplacing and biodegradable materials, respectively. The biodegradable or bioreplacing property is related to the solubilities of these ceramic materials. The solubility depends on the crystal structure and specific surface area, and so on [13]. Since the crystal structure of the metastable phase is different from the calcium phosphate ceramics and the metastable phase appears in the surface of the Ca-def HAp crystals, the presence of the metastable phase affects for the solubility of the calcium phosphate ceramics. The findings in the present study are expected to contribute to the development of high performance biomaterials.

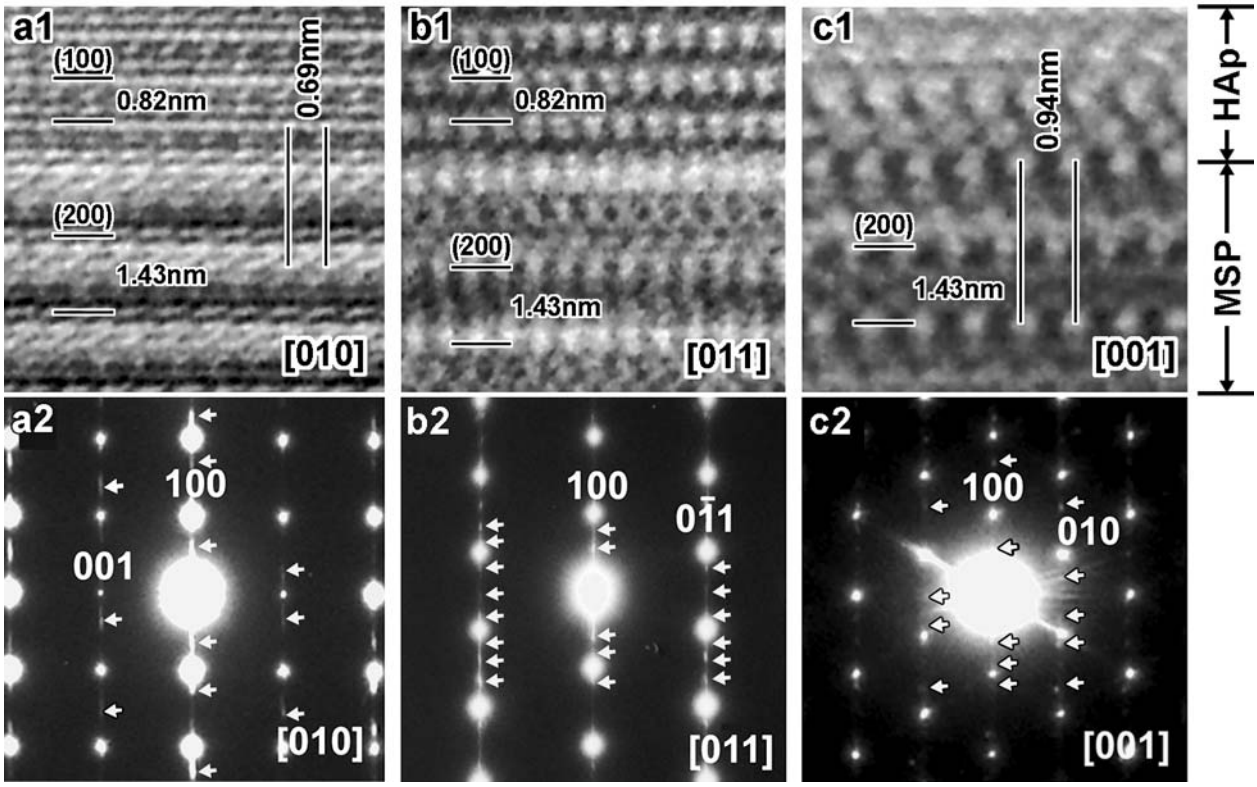

Figure 7 HRTEM images of a Ca-rich metastable phase (a1, b1 and c1) and its electron diffraction pattern (a2, b2 and c2). Several diffraction spots from the metastable phase (MSP) shown by arrows.

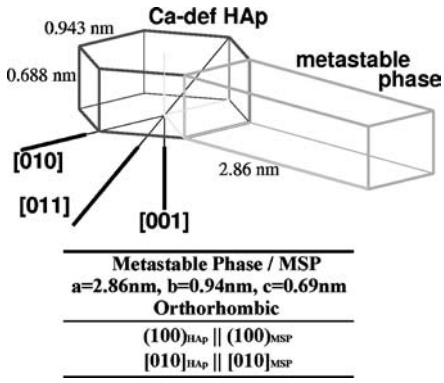

Figure 8 Crystallographic relationship between HAp matrix and a metastable phase (MSP).

4. Summary

In the present study, we investigated the formation process of a metastable phase and the crystallographic relation between the metastable phase and the HAp matrix by HRTEM. Our results in this study can be summarized as follows:

1. From the TEM image of Ca-def HAp before annealing, several HAp whiskers with different aspect ratios agglomerated. The metastable phases grew thicker by annealing for a long period of time, and the phase grew toward the surface from the inside of the HAp matrix. By HRTEM observation, it was revealed that Ca-rich metastable phases are formed by migration to the interface and continuous accumulation of calcium ions from a HAp crystal with a small aspect ratio that is located on a large HAp whisker.

2. From HRTEM images and the results of the analysis of SAED patterns, the lattice constants of the metastable phase were determined $a = 2.86$ nm, $b = 0.943$ nm, and $c = 0.69$ nm in the orthorhombic crystals system. With respect to the relation between the HAp matrix and the metastable phase, the length of the *b*-axis and *c*-axis in the metastable phase agreed with that of the *b*-axis and *c*-axis in the HAp matrix, respectively, and the (100) plane of the metastable phase ran parallel to (100) plane of the HAp matrix.

References

1. A. S. POSNER, *Physiol. Rev.* **49** (1969) 760.
2. H. MONMA, S. UENO, Y. TSUTSUMI and K. KANAZAWA, *J. Ceram. Soc. Jpn. (Yogyo-Kyokai-shi)* **86** (1978) 590.
3. I. R. GIBSON, I. REHAMAN, S. M. BEST and W. BONIFILD, *J. Mater. Sci. Med.* **12** (2000) 799.
4. L. L. HENCH, *J. Am. Ceram. Soc.* **74** (1991) 1487.
5. A. NAKAHIRA, M. TAMAI, K. SAKAMOTO and S. YAMAGUCHI, *J. Ceram. Soc. Jpn.* **108** (2000) 99.
6. M. TAMAI, S. MIKI, G. PEZZOTTI and A. NAKAHIRA, *ibid.* **108** (2000) 915.
7. L. YUBAO, C. P. A. T. KLEIN, S. VANDEMEER and K. DEGROOT, *J. Mater. Sci. Med.* **5** (1994) 263.
8. H. MONMA, S. UENO and K. KANAZAWA, *J. Chem. Tech. Biotechnol.* **31** (1981) 15.

9. J. J. P. VALDES, J. O. LOPEZ, G. R. MORALES, G. P. MALAGON and V. P. GORTCHEVA, *J. Mater. Sci. Med.* **8** (1997) 297.
10. V. B. ROSEN, L. W. HOBBS and M. SPECTOR, *Biomaterials* **23** (2002) 725.
11. M. TAMAI, M. NAKAMURA, T. ISSHIKI, K. NISHIO, H. ENDOH and A. NAKAHIRA, *J. Mater. Sci: Mater. Med.* **14** (2003) 617.
12. A. NAKAHIRA, K. SAKAMOTO, S. YAMAGUCHI, M. KANENO, S. TAKEDA and M. OKAZAKI, *J. Am. Ceram. Soc.* **82** (1999) 2029.
13. J. C. ELLIOTT, in "Structure and Chemistry of the Apatite and Other Calcium Orthophosphates" (Elsevier, Tokyo, 1994) p. 1.

Received 19 October 2004
and accepted 20 May 2005